Vol. 83 (1993) ACTA PHYSICA POLONICA A No. 4

PHENOMENOLOGICAL VERSUS MICROSCOPIC INTERPRETATION OF INCOMMMENSURATE SYSTEMS — BCCD AND THE ANNNI-MODEL

G. SCHAACK

Physikalisches Institut der Universität Würzburg
Am Hubland, 8700 Würzburg, Germany

(Received October 5, 1992; revised version January 5, 1993)

Phenomenological and microscopic models to treat modulated crystal structures are reviewed. Their applicability to interpret the specific phase diagram of betaine-calciumchloride-dihydrate (BCCD), which is of the "incomplete devils's staircase" type, is critically discussed. Some experimental observations, which emphasize the fractal topology of the BCCD phase diagram, have been compiled. They support the preference of microscopic approaches as the ANNNI-model over the classic Landau theory for this specific case.

PACS numbers: 64.60.–i, 64.70.Rh, 77.80.Bh

1. Introduction

Incommensurate crystal structures have attracted considerable activities in solid state science because these systems can be regarded physically as an intermediate between the crystalline and non-crystalline state. In general, incommensurate (ic) phases are encountered before the crystal transforms from a paraelectric (disordered) state (n) to an ordered (ferroelectric (fe) or ferroelastic) phase at low temperatures or they are intercalated between commensurately (c) modulated phases of varying modulation wave vectors. The essential feature of a crystal in the ic state is the modulation of the crystal structure with a wavelength of the order parameter, which is irrational to the existing lattice period and which changes continuously with an external parameter, e.g. temperature T or pressure p. In the c phases the modulation locks in at a rational multiple p of the lattice period with a p-fold increase in the unit cell. A sequence of several lock-in phases may be encountered before the system finally enters the low temperature phase. In the ic phase the system has no translational symmetry but it has, of course, long-range

order. Its X-ray diffraction patterns show sharp spots that have to be labelled by more than three Miller indices.

Sequences of differently modulated c phases interrupted by ic phases have been studied theoretically in detail by various methods [1], they are called an "incomplete devil's staircase". This peculiar type of behaviour is well represented by BCCD (betaine-calciumchloride-dihydrate, $(CH_3)_3NCH_2COO{\cdot}CaCl_2{\cdot}2H_2O$; $D_{2h}^{16}(Pnma)$, $Z = 4$ at $T = 300$ K). BCCD is an addition compound of the α-amino acid betaine and the inorganic component. Many features of its unusual properties have been investigated in the last few years [2]. At $T_I = 164$ K the ic state is encountered (second-order transition) with the one-dimensional modulation $q = \delta(T)c^*$, $\delta(164\text{ K}) = 0.32$. With lowering T, δ decreases continuously. Prominent c phases with $\delta = m/p = q_i/|c^*|$ (m, p — integer, q_i — wave vector of one-dimensional modulation along c^*) are $\delta = 2/7$ ($127.8 \geq T \geq 124.5$ K), 1/4 ($115.3 \geq T \geq 75.8$ K), 2/9, 1/5, 2/11, 1/6, 2/13, 1/7, 1/8, 0/1 (fe) at $T \leq 46.0$ K ($P_{fe} || b$) [2, 3]. Details, more c phases at ambient pressure, and the ic phases sandwiching the c phases in the interval ($164\text{ K} \geq T \geq 115.3$ K) can be found in [3].

In the following we review shortly the theoretical procedures used to describe devils's staircase systems: the phenomenological Landau approach, and the microscopic treatments based on statistical theories of Ising-type pseudo-spins. The prototype of the latter methods is the ANNNI-model (axial next-nearest neighbour Ising, [1]). In the next section experimental results will be compiled, mainly from spectroscopic and dielectric work done at Würzburg, which support the conclusion reached that much of the physics occurring in BCCD is in surprisingly good agreement with the predictions of this microscopic approach.

2. The Landau theory of c and ic phases

Many authors have contributed to a rather complete understanding of the normal → incommensurate (n→ic) type of transition into the ic state and, at lower temperatures, into the lock-in (c) phase in the frame of the classical Landau approach [4, 5]. For δ along z, the order parameter Q is complex: $\{Q(k),\ Q^*(-k)\}$, $Q = Pe^{i\Phi(z)}$, Q is spatially varying. Expanding the thermodynamic potential $f(z)$ in terms of Q, Q^* delivers the term $A(T)QQ^*$ and higher powers of Q, Q^*, but also the Lifshitz invariant $Q(\partial Q^*/\partial z) - Q^*(\partial Q/\partial z)$ and higher order invariants of Q, $\partial Q/\partial z$, $(\partial^2 Q/\partial z^2)$ and others. The symmetry of the high temperature phase determines which of these invariants enter $f(z)$. Near T_I, the plane-wave approximation is generally valid: $\Phi = \text{const}\cdot z$, $dP/dz = 0$ (sinusoidal modulation). While in most ic materials the modulation squares with decreasing T, as in thiourea, i.e. higher harmonics of the modulation grow and higher order satellites are observed in X-ray diffraction, surprisingly no such squaring is found in BCCD [6].

A free-energy density $f(z)$, verifying all symmetry constraints of BCCD, has been used by Ribeiro et al. [7] to take the transition at T_I and the most prominent lock-in transitions into account

$$f(z) = \frac{\alpha}{2}P^2 + \frac{\beta}{4}P^4 - \frac{\sigma}{2}\left(\frac{\partial P}{\partial z}\right)^2 + \frac{\gamma}{4}\left(\frac{\partial^2 P}{\partial z^2}\right)^2 + \nu P^2\left(\frac{\partial P}{\partial z}\right)^2. \qquad (1)$$

$\alpha = \alpha_0(k)(T - T_0)$; α_0, β, γ, $\sigma > 0$. The averaged free-energy density F is $F = L^{-1} \int_0^L f(z)\mathrm{d}z$. L is the pitch of the modulation. The coefficients σ and γ are chosen in order to describe the occurrence of modulated structures, since the terms associated with these coefficients are responsible for a minimum in the dispersion curve $\alpha_0(k)$ at an arbitrary point q of the Brillouin zone, $q = \delta c^*$. The dispersive term $\nu P^2(P_z)^2$ imposes a temperature dependence of q_i [7]. For taking the various lock-in phases into account, the existence of additional "umklapp" terms ($\propto P^{2p}$, $\delta = m/p$) in the free-energy density $f(z)$ is required. To avoid the uncomfortably high powers of P involved ($p \leq 23$, see Sec. 4), an adjustable β_{eff} was introduced ad hoc in (1) [7]. With this phenomenological model, the main features of the complex behaviour of BCCD at ambient pressure can be taken into account.

The coefficients α, β, σ, etc. can be determined either by adjustment to experimental data, as in [7], or by derivation from a microscopic model of the anharmonic single-particle and the two-particle interaction potential up to the fourth order [8, 9]. The latter procedure, which is conceptually more satisfying, may result in a Landau expansion of $f(z)$ up to high orders of umklapp terms, where the coefficients are derived in a unique manner from the few parameters of the microscopic model. This model has not yet been applied to BCCD. Problems may arise, because this treatment requires the presence of secondary order parameters (higher harmonics of the modulation) for the location of the c phases.

There has been an intense but speculative search for another (second) order parameter in BCCD which is not responsible for the modulation but for a possible small monoclinic distortion, starting with the theoretical work of Dvořák [10] and the detection of a slight rotation of the indicatrix below T_{I} [11]. A careful evaluation of all available experimental data [12], however, favours a model with only one order parameter at least in the temperature region above 70 K.

3. Predictions of the ANNNI model for BCCD

The ANNNI-model [1] considers a primitive tetragonal lattice of Ising pseudo-spins oriented along the tetragonal (z-) axis, the axis of modulation. In the planes $\perp z$ the spins $S_{i,j}$ and $S_{i,j\pm1}$ are fe coupled to their nearest neighbours with an interaction energy J_0. Nearest neighbours (NN; i, $i \pm 1$) along z are either fe coupled ($J_1 > 0$) or antiferroelectrically (afe) ($J_1 < 0$), while next-nearest neighbours (NNN; i, $i \pm 2$) along z are assumed to be afe coupled ($J_2 < 0$). The Hamiltonian of this model may be written as

$$H_A = J_0 \sum_{i,j} S_{i,j} S_{i,j+1} - J_1 \sum_{i,j} S_{i,j} S_{i+1,j} - J_2 \sum_{i,j} S_{i,j} S_{i+2,j}. \tag{2}$$

The parameter $\kappa = -J_2/J_1$ is introduced, $\kappa \neq 0$, the sign of κ depends on the sign of J_1. For both signs of κ frustrated interactions (fe versus afe) will occur and give rise to modulated structures [13]. The model is controlled by only two adjustable parameters $k_{\text{B}}T/J_0$, κ.

A part of the mean-field phase diagram of the ANNNI-model in Fig. 1 shows the paraelectric (p), fe phase and the c phase ($\delta = 1/4$), enclosing the region of

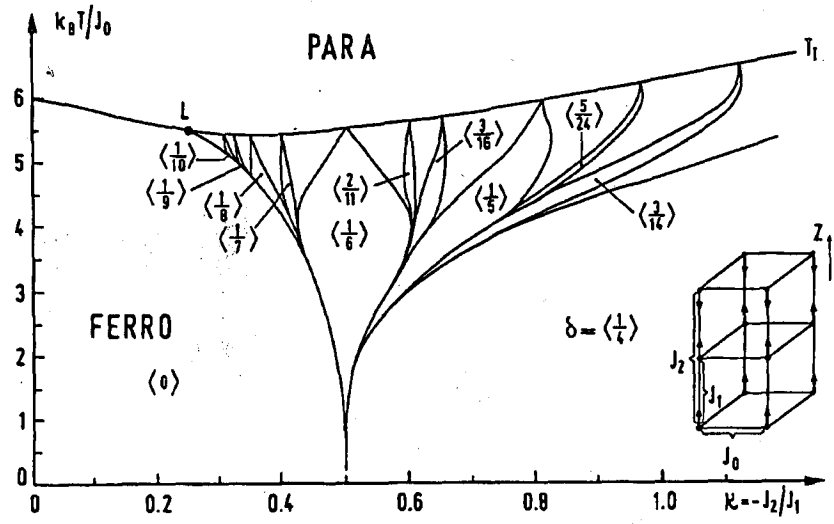

Fig. 1. Mean-field phase diagram of the ANNNI-model [14], showing the region of the modulated phases ("devil's flower"); L — Lifshitz point, δ in units of $|c^*|$. The inset (right) depicts the tetragonal Ising-spin lattice of the ANNNI-model, modulation q along z.

more complicated c and ic modulated phases. The c phases display shapes like leaves of the devil's flower with the tips ending at T_I. Due to entropic effects not considered here, successive c phases of high order will be replaced by ic phases with δ varying continuously. A Lifshitz (multicritical) point occurs near $\kappa = 0.25$. We refer to the fact that the line, which separates the p phase from the modulated phases ("T_I-line", near $k_BT/J_0 = 5.5$), depends only weakly on κ, while the phase boundaries between the various c phases are strongly governed by κ. In linearized mean-field theory, the critical wave vector q_i and the T_I-line can be calculated in closed form [14]

$$q_i = q(\kappa, T_I) = \cos^{-1}(1/4\kappa); \tag{3}$$

$$k_BT_I(\kappa) = 4J_0 + J_0\left[2\kappa + (4\kappa)^{-1}\right], \qquad (\kappa \geq 0.25). \tag{4}$$

For the other phase boundaries (between the c phases) expressions in closed form are not available.

Detailed theoretical studies of the ANNNI-model have revealed the existence of structure combination branching processes (bifurcations) and accumulations of these processes in certain well-defined regions of the c phases [1, 13, 14]. In a structure branching process between two c phases with $\delta_1 = i/j$ and $\delta_2 = k/l$ a new c phase develops with a modulation vector $\delta_b = (i+k)/(j+l)$. With T and (or) κ changing, these branching processes will proceed to $\delta_{b,n} = (i+nk)/(j+nl)$, $n \in N_0$. As the stability of phases (i.e their width in Fig. 1) with complicated modulation patterns decreases, the density of c phases with increasing complexity will grow towards an "accumulation point" (AP, $n \to \infty$) in the (κ, T)-phase diagram. These structure branching processes and their accumulations appear as characteristics

for modulated phases which follow the ANNNI-model. This model gives detailed predictions for the occurrence of these "fractal structures" in the phase diagram. Results of other, more elaborate microscopic models on these effects are not yet available [15, 16]. These models also start from an ansatz for the anharmonic molecular potentials similar to the potentials used for the Landau approach. Thus both methods obviously share a common basis. The Landau approach, however, has not yet been analysed for its potential to take the fractal properties of the phase diagram of BCCD and their consequences into account.

4. Experimental results on BCCD

In this chapter a selection of experimental results is given, which emphasize the fractal character of the phase diagram of BCCD. An important experimental parameter besides temperature is the application of external pressure, both hydrostatic and uniaxial, because the interaction parameters (J_i of the ANNNI-model or of the anharmonic potentials) can be varied by the pressure dependence of the interatomic distances in a quasi-controlled manner. We have performed detailed studies of the temperature and pressure dependence of the dielectric constant $\varepsilon(p,T)$ in the ranges of 20 K $\leq T \leq$ 300 K and 0.1 $\leq p \leq$ 550 MPa. The extrema of ε mark the phase boundaries at the transition temperatures T_t. The (p,T)-phase diagram of BCCD thus obtained is presented in Fig. 2 [17]. With in-

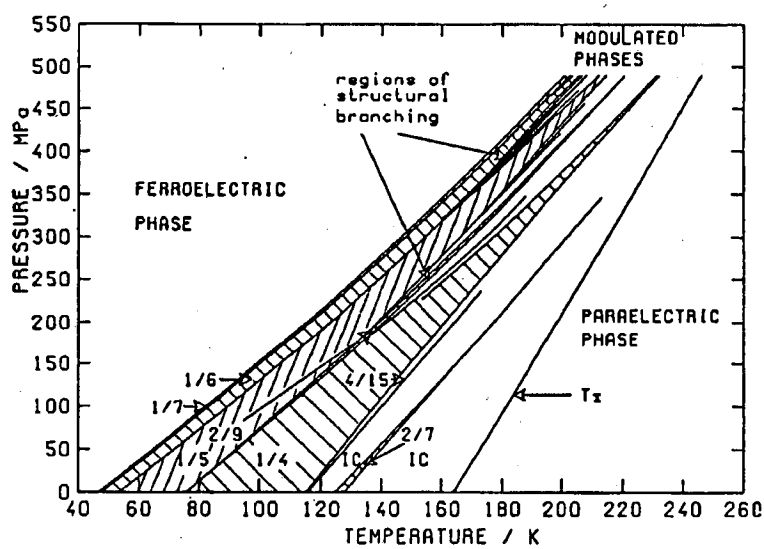

Fig. 2. (p,T)-phase diagram of BCCD [17]. Hatched areas — c phases with δ-values given; blank areas in the modulated region — ic phases.

creasing pressure all ic and c phases are stabilized, $(dT_t/dp) > 0$, the interval ΔT of stability is near T_I generally decreasing. A Lifshitz point L can be extrapolated near $T_L = 346$ K, $p_L = 1.16$ GPa. Structure branching patterns (bifurcations) can

be observed near 150 K and 250 MPa around the $\delta = 2/9$-phase, near 180 K, 380 MPa ($\delta = 2/11$) and (unresolved) near 200 K, 500 MPa (2/13). The plethora of c and ic phases near $\delta = 2/7$ can be interpreted as the aftermath of a branching occurring at negative pressures and close to 100 K. Fractal properties of the phase diagram (self-similarity) are clearly discernible [17] within the branching regions, where narrow c phases are in general sandwiched by reentrant ic phases, which will dominate the diagram with T and p finally approaching L. An experimental proof for the existence of these reentrant ic phases, which are not observed at ambient pressure, is found in Fig. 3. Here the pressure dependent wave number shift of a transmission maximum of BCCD in the FIR spectral region at 175 K is plotted. The branching regions at $\delta = 2/9$ and 2/11 are both crossed. Within the c phases the phonon frequencies are constant but vary continuously through the ic regions, depicting the dispersion of an acoustic phonon branch scanned by the δ-dependent zone boundary due to the folding of the Brillouin zone [18].

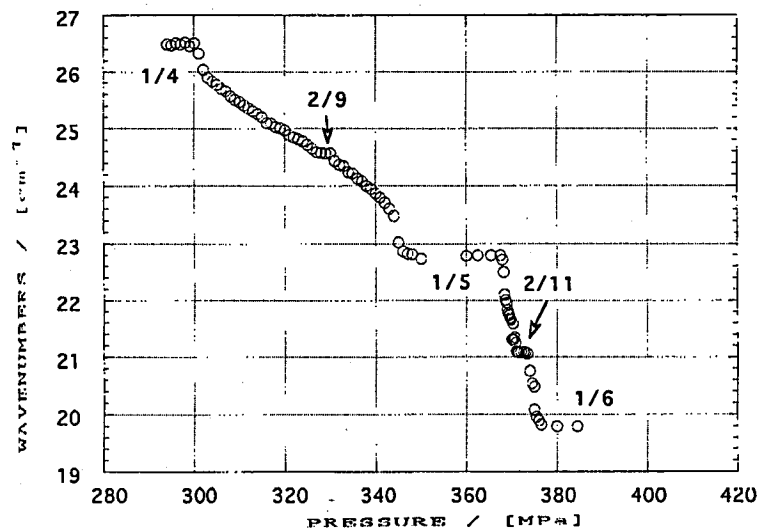

Fig. 3. Pressure dependent wave number shift of a transmission maximum in the FIR absorption spectrum of BCCD, ($\boldsymbol{E} \parallel y$, sample thickness $\approx$ 150 μm) taken along the isotherm at $T = 175$ K, which intersects two structure branching regions (near $\delta = 2/9$ and $\delta = 2/11$). c phases with δ-values indicated are characterized by frequencies independent on p, ic phases demonstrate continuously varying frequencies [18].

Negative pressure, i.e. an expansion of the unit cell, can be realized by substituting ions with larger ionic radii on regular lattice sites ("chemical pressure"). This has been achieved in BCCD by introducing a small percentage of Br^- on Cl^--sites and the opposite behaviour by a $Mn^{2+} \rightarrow Ca^{2+}$ substitution. With Br^--doping, all T_t shift to lower temperatures, an averaged chemical pressure of 10.1 MPa/(% Br^-) has been observed [19]. In addition the local lattice strain at

the Br^- sites causes pinning of the modulation with increasing hysteresis effects as a consequence, (the c→c transitions are of the first order). With growing concentration more and more phases with long-period modulation are suppressed and a glass-like freezing of a relaxatory dipolar motion is found. Remember that the prerequisite of the glassy state are the frustrated interactions, clearly effective in BCCD.

If we follow the size of the dielectric anomalies along a phase boundary, say $\delta = 2/9 \rightarrow 1/4$ or ic, we observe first a strong increase of ε with growing p, then a broad maximum is found, generally occurring in the branching region, and finally a gradual decrease will be registered until the anomaly disappears (Fig. 4), [20]. We have attributed these maxima of ε and, consequently, of the Curie constant to

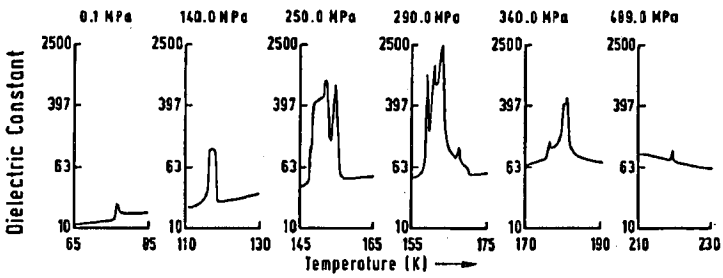

Fig. 4. Dielectric anomalies of BCCD in a logarithmic scale at various hydrostatic pressures in the region of structure branching processes between the $\delta = 1/4$- and $\delta = 1/5$-phases. The anomaly at 489 MPa is due to the narrow 2/9-phase [20].

the occurrence of an AP of branching processes. ε near the AP is enhanced up to a factor of 250 over the size of the anomaly measured outside the branching region. Although the high order c phases near an AP do not exist as stable phases, they contribute to the fluctuations of the order parameter. The extrema of ε thus locate the positions of the AP in the (p,T)-phase diagram. In Table I we have compiled the observed AP, they compare surprisingly well with the position expected by the ANNNI-model [13, 14]: $T_{\mathrm{AP}}^{\mathrm{ANNNI}} \approx 159$ K.

Experiments applying uniaxial pressure should indicate, why BCCD so closely follows the predictions of a simple model as the ANNNI-model is. Under such experimental conditions the intermolecular interactions causing the modulation will be varied in an easily controlled manner and the results can be compared with the effects due to a uniaxial deformation of the pseudo-spin lattice of the ANNNI-model, assuming a growing interaction strength with reduced spin distances. Uniaxial pressure F was applied along the x-, y-, z-axis of orthorhombic BCCD, while the phase transition temperatures were determined by observing the dielectric anomalies (ε_y) in the y-direction. In Table II the slopes $(\partial T_t/\partial p_x|_{p=0}$ etc.) have been compiled and compared with the results of hydrostatic pressure. Obviously the crystal behaves considerably different under uniaxial or hydrostatic

TABLE I

Locations of accumulation points in the (p,T)-phase diagram of BCCD between the $\delta = 1/4$ and $\delta = 1/5$ c-phases, and maxima of fitted Curie constants $C_j(T_{AP})$ [20].

Phase transit. (δ)	T_{AP}/K	p_{AP}/MPa	C_j/K
(1/5 ...) ic – 2/9	151.8	246.5	158
2/9 – ic (...1/4)	151.3	236.3	170
ic – 3/14 – ic	151.5	246.5	4.4
ic – 4/19 – ic	158.1	274.4	11.4
1/5 – ic	160.0	281.0	14
ic – 3/13 – ic	149.8	230.4	6.8
ic – 4/17 – ic	150.6	227.3	13.5
ic – 1/4	150.6	225.3	8

TABLE II

Observed derivatives of phase transition temperatures T_i in BCCD with uniaxial pressure (p_x, p_y, p_z) and hydrostatic pressure p (K/MPa) [17, 21].

Transition, T [K]	$\partial T_i/\partial p_x$	$\partial T_i/\partial p_y$	$\partial T_i/\partial p_z$	$\partial T_i/\partial p$
T_i, 164	+0.031±0.065	+0.053±0.032	−0.008±0.098	+0.176
ic ↔ $\delta = 2/7$, 128	+0.037±0.080	−0.009±0.035	+0.160±0.093	+0.250
$\delta = 2/7$ ↔ ic, 125		−0.022±0.033		+0.286
ic ↔ $\delta = 4/15$, 116	+0.009±0.083	−0.043±0.033	+0.22±0.10	+0.243
$\delta = 1/4$ ↔ 1/5, 75	±0.00±0.11	−0.010±0.038	+0.30±0.12	+0.302
$\delta = 1/5$ ↔ 1/6, 53	±0.00±0.12	+0.006±0.042	+0.34±0.18	+0.368
$\delta = 1/6$ ↔ 0, fe, 46	−0.03±0.12	−0.033±0.041	+0.28±0.13	+0.359

pressure: Only small effects are observed for $F \parallel x$ or y with either positive or negative slopes $\partial T_t/\partial p_{x,y}$. At $F \parallel z$ (the direction of the modulation in BCCD) the lock-in phases shift linearly and roughly with the same slopes as under hydrostatic pressure. The transition at T_i, however, displays only small shifts, irrespective of the direction of F, and different from the behaviour under hydrostatic pressure. For the ease of interpretation the results have been transformed from the stress dependencies of the transition temperatures to their strain dependencies: $\partial T_t/\partial p_{x,y,z} = \partial T_t/\partial \sigma_{1,2,3} \rightarrow \partial T_t/\partial \varepsilon_{1,2,3}$, using the known elastic constants (stiffnesses) $c_{i,j}$ of BCCD (in Voigt notation). This procedure eliminates the effects of lateral strains on the transition temperatures and provides results, which are directly comparable with the uniaxial deformation of the pseudo-spin lattice

(Fig. 1), and which indicate that the transition (n → ic) at T_I depends strongest on a lattice deformation along the x-direction. Next in importance is the y-direction, while a deformation along z is of minor relevance. The transitions into the lock-in phases $\delta = 2/7$ and $\delta = 4/15$ display the opposite hierarchy of deformations. Here the strain along the axis (z) of the modulation is most important, while ε_1 has the least effect. This trend becomes even more pronounced for c phases at lower temperatures.

These results are in full agreement with the predictions of the ANNNI-model, as is evident from Fig. 1 and Eq. (3): The T_I-line in the figure runs almost horizontally at $k_B T/J_0 \approx 5.5$ and depends only marginally on $\kappa = -J_2/J_1$. An increase in the inplane coupling constant J_0, as caused by a uniaxial compression of the crystal along the x- or y-directions, will shift T_I to higher temperatures more effectively than an increase in κ due to a deformation along z. The opposite is true for the (c↔c)-transitions, as is again evident from Fig. 1. Here the phase boundaries between c-phases (near the Lifshitz point) are oriented almost parallel to the $k_B T/J_0$-axis, i.e. they are strongly dependent on κ, but almost unaffected by the size of J_0. Thus the largest effect on the c-phases is expected from a strain ε_3 along the modulation axis, as is indeed observed in BCCD.

The question raised, why BCCD obeys the predictions of the ANNNI-model so well, can be answered now in parts as follows: Although the pseudo-spins of the ANNNI-model cannot be located at present in the BCCD lattice nor attributed to specific molecular units in this material, the scheme of intermolecular interactions effective in this crystal is closely correlated to the assumptions underlying the ANNNI-model (J_0, J_1, J_2, J_1/J_2 occurring with both signs).

5. Conclusions

BCCD is one out of a few materials where both the phenomenological and a microscopic theory have been elaborated to interpret the phase sequence [7, 13, 16]. Both procedures have their merits and their drawbacks: The Landau approach is an expansion of the free energy in terms of the order parameter at the n→ic phase transition with invariants adapted to n-phase symmetry. Competing interactions are taken into account by the opposite signs of the order-parameter derivatives in (1): $\{(\sigma/2)(\partial P/\partial z)^2 < 0, (\gamma/4)(\partial^2 P/\partial z^2)^2 > 0\}$, see [7]. It can be expected that the n→ic transition and the subsequent transition into the first c phase are well represented by this method (transition from the plane-wave region to the discommensuration (soliton) regime [4] close to the first ic→c transition, where nearly commensurate domains in the crystal are separated by domain walls (discommensurations, solitons), where all the incommensurability is localized). Additional c→c transitions, however, and especially (c→ intermittend ic)-phases are difficult to model and require an unreasonable large number of adjustable parameters, which cannot be based on physical argumentation, or a reliable model of single particle and intermolecular potentials. It provides however standard methods for calculating thermodynamic potentials, variables and all kinds of susceptibilities.

The discrete spin models, i.e. the ANNNI-model and its derivatives, on the other hand, have as ground states well ordered ferroelectric ($\delta = 0/1$) or modulated

phases (e.g. $\delta = 1/4$ and many others, perhaps degenerate). Most investigations have to rely on a time consuming numerical analysis, analytical results are scarce. Opposite to the Landau approach, the behaviour at higher temperatures has to be derived from the fully squared groundstates, in most cases in a mean-field approximation (MFA), where the spins in a plane $j \perp z$ have an average value $\overline{s}_j < 1$. For high temperatures the n-phase ($\overline{s}_j = 0$) is the only solution. At decreasing temperatures an instability occurs for $\kappa > 1/4$ at a wave vector given by (2). Below that transition many narrow c phases with distinct δ-values ($\delta = m/p$) with large p, $p+1$, . . are encountered (Fig. 1), which sometimes are difficult to distinguish from an ic phase with δ varying continuously. The ANNNI-model has been used recently by Siems and Tentrup [13] to interpret the observed sequence of modulated phases in BCCD and the branching points by adjusting the interaction parameters of the model. Their result is presented in Fig. 5. To correlate the (p–T)-values of Fig. 2 with the ANNNI-interaction constants J_0, $-J_1/J_2 = \kappa^{-1}$ of Fig. 5, the fact was used that the $\delta = 1/6$-phase is centred around $\kappa^{-1} = 2$ (Fig. 2). The other c-phases are shifted parallel until their (extrapolated) tips

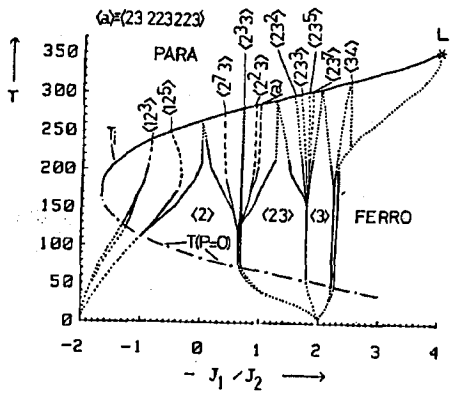

Fig. 5. ANNNI- type phase diagram of BCCD in the T vs. $J_1/|J_2|$ representation as constructed from Fig. 2 by Siems and Tentrup [13]. Full lines — phase boundaries in the experimentally covered (p–T)-range; dotted lines — extrapolation to the T_I-line or to the ($T = 0$ K)-line, respectively. The wave vector δ corresponding to a c-structure $\langle n_1, n_2, \ldots n_j \rangle$ is $\delta = 0.5j/\sum_{i=1}^{j} n_i$. $\langle n_1, n_2, \ldots n_j \rangle$ indicates a c-structure, where the Ising spins in n_1 neighbouring basal planes are oriented up, in the n_2 next planes down, n_3 up, etc.

intersect the T_I-line at q-values determined experimentally in [17]. The region of negative pressure is extrapolated to the positions of the various phases predicted by the ANNNI-model (Fig. 2). The experimental phase diagram agrees nicely with the properly adjusted ANNNI-diagram. There are, however, quantitative differences, which might be due to a MFA overestimate of the stability of c-phases and the fact demonstrated in Tab. II that pressure affects J_i with different strength.

Whenever the "incomplete devil's staircase", i.e. the fractal topology of the phase diagram is considered, a microscopic spin model analysis has to be preferred

over the phenomenological treatment. This becomes more evident when we study the mapping of the spin averages $\overline{s}_j$, j labelling subsequent basal planes of the pseudo-spin lattice (Fig. 1) [1, 13]

$$\overline{s}_{j+2} = \tilde{H}(\overline{s}_{j-2}, \overline{s}_{j-1}, \overline{s}_j, \overline{s}_{j+1}) \tag{5}$$

by a symplectic matrix $\tilde{H}$, derived from (2) in MFA [13]. If $\overline{s}_{j-2}, \ldots, \overline{s}_{j+1}$ are known, $\overline{s}_{j+2}$ can be calculated. A c-phase corresponds to a polarization profile $\{\overline{s}_{j-2}, \ldots \overline{s}_{j+2}\}$, which repeats itself after a finite number of steps. One then obtains a discrete mapping permitting iterated fixed point expansions that can be interpreted as a *spatial* analogue with κ as a control parameter to the evolution of a discrete nonlinear dynamical system in the *time* domain [16]. Several results of this tremendously developing field can then be used, especially the branching (bifurcation) route and the route to deterministic chaos towards an accumulation point [22].

The simple spin models suffer from a serious drawback: Methods and models for constructing equilibrium equations, free-energy functionals and for calculating susceptibilities, which are standard in the Landau approach and can be obtained in closed form, are difficult to develop or are not yet available but are urgently needed. More advanced models, combining important advantages of both methods, have been sketched recently [15, 16], but are not yet analysed as completely as the simple ANNNI-model. Future work in these directions should improve this situation.

Acknowledgments

The Deutsche Forschungsgemeinschaft has supported some of these investigations. The author is grateful to many graduate students, who have successfully and with great enthusiasm contributed to this project, and especially to M. Schmitt-Lewen for a critical reading of the manuscript.

References

[1] For reviews see: S.Aubry, in: *Solitons and Condensed Matter*, Eds. A.R. Bishop, T. Schneider, Springer Series in Solid-State Sciences **8**, 264 (1978); P. Bak, *Rep. Prog. Phys.* **45**, 587 (1982); T. Janssen, A. Janner, *Adv. Phys.* **36**, 519 (1987); W. Selke, *Phys. Rep.* **170**, 214 (1988); W. Selke, in: *Phase Transitions and Critical Phenomena*, Eds. C. Domb, J.L. Lebowitz, Vol. **15**, 1 (1992).

[2] J. Albers, *Ferroelectris* **78**, 3 (1988); G. Schaack, *Ferroelectrics* **104**, 147 (1990).

[3] H.-G. Unruh, F. Hero, V. Dvořàk, *Solid State Commun.* **70**, 403 (1989).

[4] A.P. Levanyuk, D.G. Sannikov, in: *Incommensurate Phase in Dielectrics I*, Eds. R. Blinc, A.P. Levanyuk, North-Holland, Amsterdam 1986, p. 1 and 43.

[5] J.-C. Tolédano, P. Tolédano, *The Landau Theory of Physe Transitions*, World Scientific, Singapore 1987.

[6] F.J. Zuñiga, J.M. Ezpeleta, J.M. Pérez-Mato, W. Paciorek, G. Madariaga, *Phase Transitions* **31**, 29 (1991); M.R. Chaves, private communication.

[7] J.L. Ribeiro, J.-C. Tolédano, M.R. Chaves, A. Almeida, H.E. Müser, J. Albers, A. Klöpperpieper, *Phys. Rev. B* **41**, 2343 (1990).

[8] K. Parlinski, K.H. Michel, *Phys. Rev. B* **29**, 396 (1984).

[9] K. Parlinski, *J. Phys. C, Solid State Phys.* **18**, 5667 (1985).

[10] V. Dvořák, *Ferroelectrics* **104**, 135 (1990).

[11] J. Kroupa, J. Albers, N.R. Ivanov, *Ferroelectrics* **105**, 345 (1990).

[12] H. Wilhem, H.-G. Unruh, *Z. Kristallogr.* **195**, 75 (1991).

[13] R. Siems, T. Tentrup, *Ferroelectrics* **98**, 303 (1989); ibid. **125**, 75 (1992).

[14] W. Selke, P.M. Duxbury, *Z. Phys. B* **57**, 49 (1984).

[15] T. Janssen, *Z. Phys. B* **86**, 277 (1992).

[16] Z.Y. Chen, M.B. Walker, *Phys. Rev. B* **43**, 760 (1991).

[17] R. Ao, G. Schaack, M. Schmitt, M. Zöller, *Phys. Rev. Lett.* **62**, 183 (1989).

[18] M. Illing, Diploma Thesis, University Würzburg (1992), unpublished.

[19] R. Ao, G. Lingg, G. Schaack, M. Zöller, *Ferroelectrics* **105**, 391 (1990); M. le Maire, G. Lingg, G. Schaack, M. Schmitt-Lewen, G. Strauss, *Ferroelectrics* **125**, 87 (1992).

[20] S. Kruip, G. Schaack, M. Schmitt-Lewen, *Phys. Rev. Lett.* **68**, 496 (1992); *Ferroelectrics* **125**, 69 (1992).

[21] B. Kirchner, M. le Maire, G. Schaack, M. Schmitt-Lewen, submitted to *Europhys. Lett.* (1993).

[22] H.G. Schuster, *Deterministic Chaos*, Verlag Chemie, Weinheim 1988.